Available online at www.sciencedirect.com
ScienceDirect
Surface Science 600 (2006) 3280–3284
SURFACE SCIENCE
www.elsevier.com/locate/susc

Formation of single layer h-BN on Pd(1 1 1)

M. Morscher *, M. Corso, T. Greber, J. Osterwalder

Physik-Institut, Universität Zürich, Winterthurerstrasse 190, CH-8057 Zürich, Switzerland

Received 13 April 2006; accepted for publication 15 June 2006
Available online 7 July 2006

Abstract

The structure of hexagonal boron nitride (h-BN) on Pd(1 1 1) was studied with low energy electron diffraction (LEED), photoelectron spectroscopy and scanning tunnelling microscopy (STM). h-BN forms flat monolayers on the Pd(1 1 1) surface in contrast to Rh(1 1 1) where a complex self-assembled double layer structure, the nanomesh [M. Corso, W. Auwärter, M. Muntwiler, A. Tamai, T. Greber, J. Osterwalder, Science 303 (2004) 217], appears. The LEED patterns reveal a dominating 10×10 h-BN superstructure, with a second, distinct structure rotated by 30° and further azimuthally randomly oriented h-BN overlayers. This is consistent with STM images which show several different Moiré patterns associated with different rotation angles of the overlayer. Additionally the use of thin Pd(1 1 1) films instead of single crystal substrates was studied. No significant differences in the h-BN film quality were found.

Keywords: Hexagonal boron nitride (h-BN); Palladium; Moiré pattern; Scanning tunneling microscopy (STM); Low energy electron diffraction (LEED)

1. Introduction

Ultra-thin insulating films on metallic substrates are model systems for metal–insulator interfaces and a key step in the bottom–up design of nanostructures. An attractive candidate is hexagonal boron nitride, which forms flat monolayers on many metal surfaces, as observed for Ni(1 1 1) [2], Ni(1 0 0) [3], Ni(1 1 0) [4], Pt(1 1 1) [2,5,6], Cu(1 1 1) [7] and Pd(1 1 0) [8] so far. On Ni(1 1 1), the small lattice mismatch of +0.4% between the h-BN layer and the metal surface is compensated by a slight corrugation of the adlayer. Therefore a commensurate (1×1) structure is formed, while on the other substrates coincidence lattices are observed, where the periodicity depends on the lattice mismatch. A most intriguing structure was recently observed on Rh(1 1 1) [1], where a bilayer nanomesh is formed, i.e. two layers of mesh stacked above each other such that most of the metal surface is covered.

Pd(1 1 1) has already been examined by Nagashima et al. [2] who compared the growth of h-BN on Ni(1 1 1), which they initially studied, to that on Pd(1 1 1) and Pt(1 1 1). They attributed the low energy electron diffraction (LEED) pattern to a coincidence lattice and concluded that h-BN forms flat monolayers on Pd(1 1 1). They also measured the valence band structure of h-BN for the three different substrates by using angle-resolved photoemission spectroscopy (ARPES) and found a good agreement between Ni, Pd and Pt except for the π-band of h-BN on Ni(1 1 1) which is shifted to higher binding energies.

After the discovery of the nanomesh, the question arised if rhodium was the only substrate where mesh formation is possible or if it also appeared on other substrates, maybe with different values for properties such as the mesh cell size. Therefore other transition metal surfaces were examined, among them Pt(1 1 1) [6] and Pd(1 1 1). The reason to study Pd(1 1 1) again is due to the comparable lattice mismatch with the h-BN film (−7% for Rh, −9% for Pd), and the lack of scanning tunnelling microscope (STM) data.

Our measurements confirm the results of Nagashima et al. and exclude the formation of a nanomesh-like structure. Low energy electron diffraction (LEED) and scanning tunnelling microscopy (STM) measurements show that the

* Corresponding author. Tel.: +41 44 6356691.
E-mail address: martin.morscher@physik.unizh.ch (M. Morscher).

0039-6028/$ - see front matter © 2006 Elsevier B.V. All rights reserved.
doi:10.1016/j.susc.2006.06.016

registry of the monolayer to the substrate is not unique, but that two preferred structures with different orientations are present: a 10×10 superstructure along the Pd crystallographic directions, and an incommensurate structure rotated by 30° (R30°-structure). Further Moiré patterns are present with different azimuthal rotation angles between the substrate and the BN layer.

2. Experimental

The experiments were performed in a modified VG ESCALAB 220 photoemission spectrometer [9] with a base pressure of $<5 \times 10^{-10}$ mbar, also housing a Park Instruments VPII STM [10]. The STM images are recorded with electro-chemically etched tungsten tips in the constant-current mode. All data were measured at room temperature. The experiments were performed on a Pd(1 1 1) single crystal and on twinned Pd(1 1 1)-films of 150 nm thickness grown on (0 0 0 1)-sapphire substrates. The crystal was cleaned by repeated cycles of Argon ion sputtering (15 min, 1 keV, $\sim$1.5 μA/cm^2) and exposure to O_2 (20 L) at 700 K with subsequent annealing to 1000 K, whereas the film was only briefly sputtered (3 min, 500 eV, $\sim$0.8 μA/cm^2) and annealed without any oxygen exposure.

The h-BN layers were produced by exposing the clean sample surface kept at 1000 K to 50–70 L of borazine $(HBNH)_3$. Before exposure the borazine was cleaned by freezing/melting cycles where the residual vapour in the frozen state was pumped. The coverages and the cleanliness of the samples were examined with X-ray photoelectron spectroscopy (XPS). The carbon contamination was below 1% of a monolayer.

3. Results

The LEED image (Fig. 1) shows a dominant hexagonal coincidence lattice, where a periodicity of 11×11 BN units ($a = 2.504$ Å) on top of 10×10 Pd unit cells ($a = 2.751$ Å) is derived. The spots marked with "BN" correspond to the boron nitride unit cell. Twelve BN spots are visible, where six correspond to BN units oriented along the surface directions of Pd, while the other six spots belong to a R30°-structure, where the h-BN lattice is rotated by 30° with respect to the Pd lattice. The spots are connected by a ring, indicating the presence of azimuthally rotated h-BN units. The relative intensities of both the ring and the R30°-spots vary in different preparations. A systematic dependence on the preparation conditions has not been found, i.e. neither contaminations nor other factors like $(HBNH)_3$ deposition rate and dose alone control the distribution. The influence of the sample temperature during evaporation has not been investigated systematically. The R30°-structure has also been observed for Pd(1 1 0) [8], Pt(1 1 1) [6] and Ni(1 1 0) [4]. As visible in Fig. 1, the images are threefold symmetric due to the discrimination between the different stacking sites.

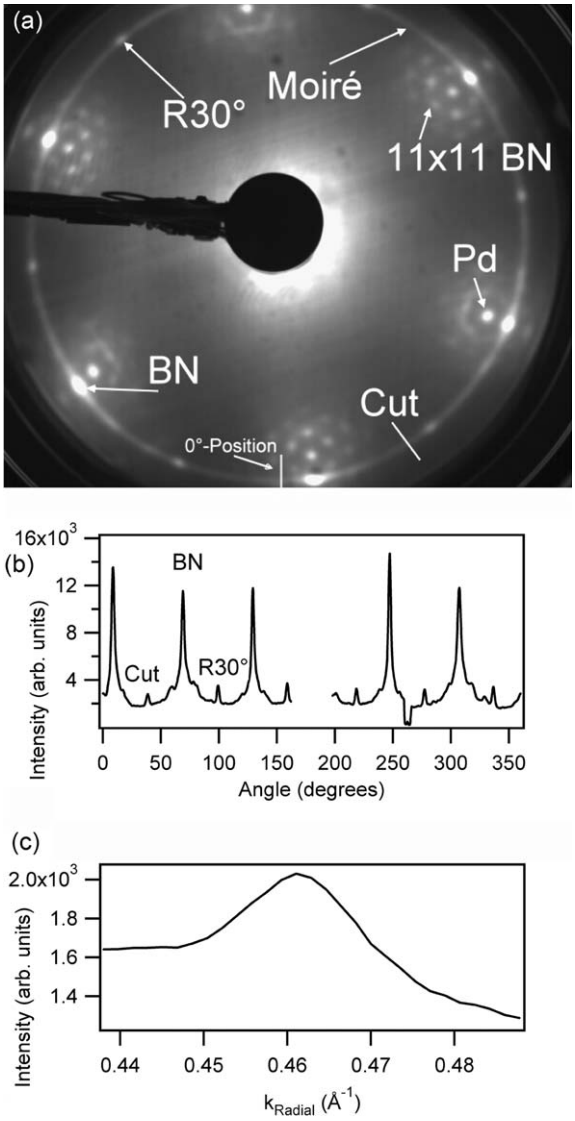

Fig. 1. (a) LEED image of the h-BN covered Pd(1 1 1) surface at $E_{kin} = 70$ eV. The Pd spots are surrounded by the BN spots and additional spots due to the coincidence lattice. Relative to the substrate spots, a 10×10 superstructure can be identified. At 30° an additional structure is found. The ring containing the BN spots corresponds to the presence of azimuthally disordered BN units on the surface. (b) A line profile along the circle containing the BN spots ($k_{radial} = 0.4611$ Å^{-1}) clearly shows these structures. The six sharp peaks marked with BN represent the BN units that are oriented along the directions of the substrate, while the six less intense peaks refer to the R30°-structure. In the region between 150° and 200° the circle is off limits of the image, and at 260° the fixation of the LEED-gun is crossed. The relative intensity of the R30°-spots and of the ring varies with preparation, but a systematic dependence has not been found. They cannot be avoided completely. (c) A cut through the circle shows the strong contribution of the randomly orientated structures, even in the presence of a strong background.

The structures found in the LEED images are also visible in the STM where several superstructures with periodicities ranging from 11 to 27.5 Å have been observed. This can be explained by Moiré patterns, i.e. the patterns resulting from the superposition of two periodic layers rotated against each other. The periodicities of the Moiré patterns arise from different rotation angles between the top h-BN

layer and the Pd substrate. Similar patterns have been observed e.g. for Pt on graphite [11]. The patterns can be reproduced by a simple overlay of two hexagonal patterns, as shown in Fig. 2. Moiré patterns have also been found on Pd(1 1 0), where in addition to the hexagonal patterns stripe-like Moirés are observed due to the rectangular symmetry of the substrate.

At atomic resolution, only one kind of the two different atoms in the h-BN lattice is imaged. For h-BN on Ni(1 1 1) this was attributed to different local densities of states (LDOS) at the Fermi level for N and B atoms at a constant height above the surface as shown by Grad et al. [12]. A higher LDOS at E_F was found for N sites, consequently N is imaged brighter than B. This is expected to apply also to Pd(1 1 1) because of the very similar band structures of the h-BN layers on the two substrates.

Concerning the corrugation of the Moiré patterns, values up to 1.6 Å have been observed. It is larger than what is expected from a purely geometrical Moiré effect, i.e. the topographic height difference between N atoms sitting on top of a Pd atom or on a hollow site. Further investigations will have to show if this enhanced corrugation is related to changes in the local work function, as it was recently put forward for other ionic overlayers on metal substrates [13,14].

The adsorption of h-BN also changes the work function, which is reduced from 5.65 eV to 4.26 eV. This value is slightly higher than the value of 4.0 eV reported by Nagashima et al. [2]. The normal emission valence band spectra are shown in Fig. 3. As shown by Nagashima et al. [2], the σ-binding energies are aligned to the vacuum level, i.e. the peak positions of the σ-bands at normal emission coincide for different substrates when referred to the vacuum level. In the case of Ni(1 1 1), the two σ-bands are degenerate at $\overline{\Gamma}$, while for Rh(1 1 1) new σ-bands appear, which are attributed to the second layer of the nanomesh [1]. The layer in contact with the metal has a higher binding energy than the one on top. For Pd(1 1 1) the spectrum is similar to Ni(1 1 1), therefore the formation of a double layer structure can be excluded. This is supported by XPS measurements. Although the h-BN coverage data exhibit large variations (the mean value of the N coverage is 1.03 ML, but the standard deviation is 0.19 ML), it is consistent with the formation of one monolayer. The similarity between Ni and Pd is also reflected in the angle-resolved photoemission spectroscopy (ARPES) data (Fig. 4), where additional bands as on Rh are again missing. One minor difference is that the σ-bands described by Grad et al. [12] for Ni(1 1 1) seem to split up on Pd(1 1 1). However, this can be traced back to a superposition of the band structures along the $\overline{\Gamma K}$ and $\overline{\Gamma M}$-directions due to the presence of the R30°-structure [4].

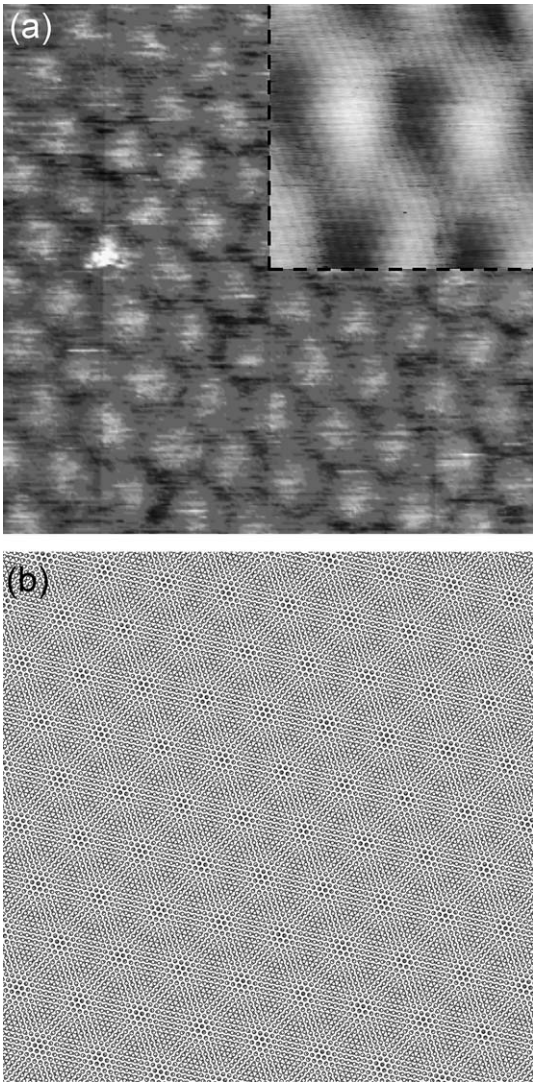

Fig. 2. (a) STM image of a Moiré pattern found on a h-BN layer on Pd(1 1 1) (20 nm × 20 nm), measured at 1 nA, 1 V. The inset in the upper right corner (2.5 nm × 2.5 nm) is measured under the same conditions and shows atomic resolution. Only one of the two atoms in the BN lattice is imaged, most probable the N atom. (b) Reproduction using an overlay of two grid patterns with lattice constants corresponding to h-BN on Pd(1 1 1). The grids are not rotated against each other, i.e. the 10 × 10 structure is shown.

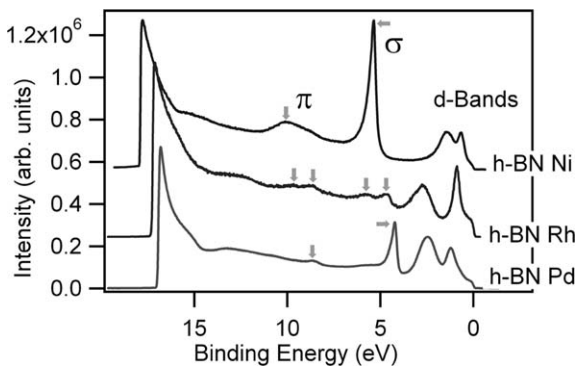

Fig. 3. HeIα ($h\nu = 21.2$ eV) excited valence band spectra at $\overline{\Gamma}$ for hexagonal boron nitride on different metal substrates. For Ni(1 1 1) the single σ-band at 5.3 eV is clearly visible. On Rh(1 1 1), an additional σ-peak arises due to the presence of two layers, where the σ-band of the layer in contact with the substrate is at higher binding energy. On Pd(1 1 1), no second band is visible.

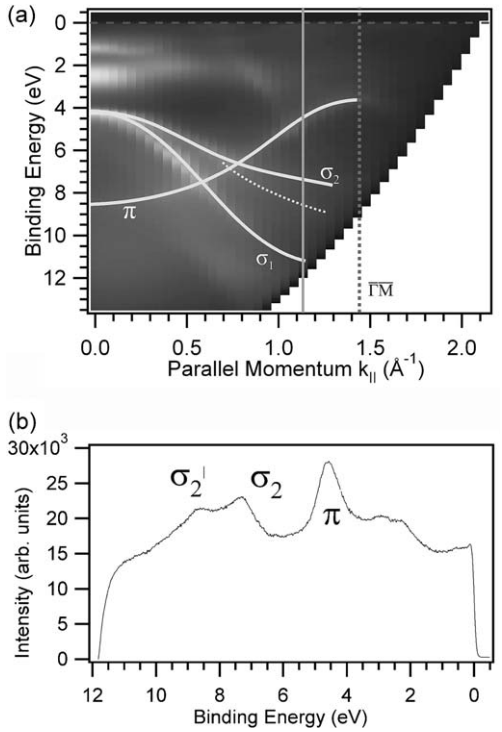

Fig. 4. (a) Angle-resolved photoemission spectroscopy (ARPES) dispersion plot ($h\nu = 21.2$ eV) of the h-BN covered Pd(1 1 1) along the $\overline{\Gamma M}$-direction of the surface Brillouin zone, corresponding to the [$\bar{2}$ 1 1]-crystallographic direction. The band structure is similar to h-BN on Ni(1 1 1) [12], indicating the formation of a single monolayer. One of the σ-bands seems to split up (the dotted line), but this can be explained by a superposition of the bands in $\overline{\Gamma K}$ and $\overline{\Gamma M}$-directions due to the presence of the R30°-structure. (b) Cut at $k_{||} = 1.13$ Å^{-1} (indicated in (a) with the vertical line). The splitting of the σ_2-band is marked with σ_2 and σ_2', where σ_2' corresponds to the σ_2-band along the $\overline{\Gamma K}$-direction.

A similar structure distribution as described above has also been observed for h-BN on Pt(1 1 1) by Müller et al. [6]. To explain the R30°-structure, they remark that for Pt(1 1 1) the BN ring diameter deviates only ~4% from the Pt lattice constant, i.e. the mismatch is reduced. Therefore they propose a model where the N atoms sit alternately on top and on bridge sites, which results in a R30°-structure. The situation is similar for Pd(1 1 1), where the mismatch between the BN ring diameter and the Pd lattice constant is 5.1%. A structure similar to the one described by Müller et al. would result in a $\sqrt{3} \times \sqrt{3}$-R30° superstructure. For clarity, the structure is shown in Fig. 5. However, no additional LEED spots are observed, therefore a compression of the layer involving a corrugation is unlikely for Pd(1 1 1). It is also worth mentioning that the mismatch for an 11×11 overstructure with the BN units rotated by 30° is only 0.36%, i.e. an additional Moiré pattern could be expected here, though it involves a corrugation as on Ni(1 1 1) [15]. Instead, the only superstructure observed in the LEED is the 10×10, due to its small lattice mismatch of 0.1%.

For the set of experiments presented above a Pd(1 1 1) single crystal was used. However, for potential applications

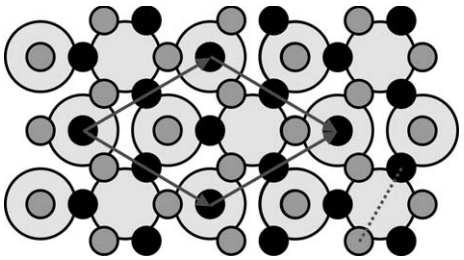

Fig. 5. Model of the $\sqrt{3} \times \sqrt{3}$-R30° structure. The black and dark grey circles represent the B or N atoms, respectively, while the light grey circles stand for the Pd atoms. The ring diameter of BN, indicated with a dotted line, deviates only 5.1% from the Pd lattice constant.

of boron nitride films cheaper alternatives are desirable. Therefore, the use of thin films of Pd(1 1 1) grown on a sapphire (0 0 0 1) substrate was examined. The films were grown on the plasma-cleaned substrate at 0.5 Å/s at ~600 °C to a thickness of 150 nm. After outgassing, annealing at 600 °C and sputtering (3 min at 500 V), LEED confirmed the growth of the (1 1 1)-orientation of Pd. The images are now six-fold symmetric because the films grow twinned, i.e. both ABC and ACB fcc-stacking occur. The six-fold symmetry is also preserved for the LEED images of the h-BN covered films (Fig. 6). It should be mentioned that the surface quality of the films is as good as that of the

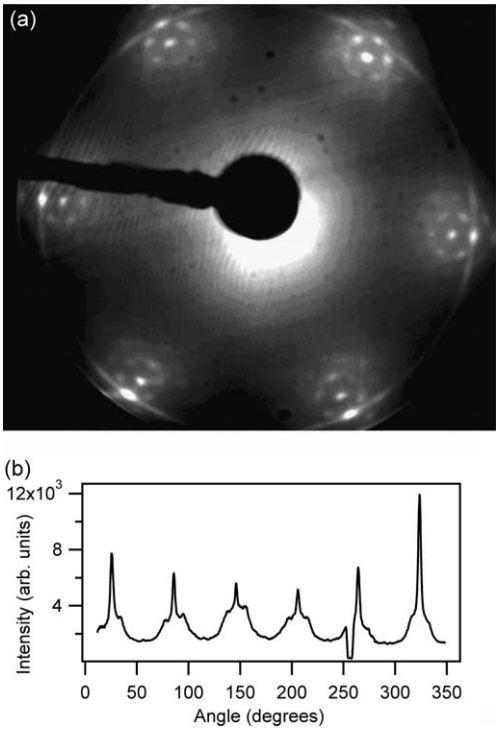

Fig. 6. (a) LEED image from the h-BN covered Pd(1 1 1) thin film at $E_{kin} = 70$ eV. The image is six-fold symmetric in contrast to the data from the crystal (Fig. 1) due to the twinned growth of the 1 1 1-surface. The rotated structure at 30° is present, but hardly visible in this LEED image, as shown in (b), which shows the intensity distribution along the BN circle (cf. Fig. 1(b)). The additional peaks close to the BN peaks are due to inplane-scattering within the BN layer. The h-BN film quality is comparable to those on the single crystal.

crystal, as judged from LEED data, apart from the symmetry difference in the images. Also the XPS and ARPES results are similar, i.e. coverages and the electronic structure differ not more than for subsequent preparations on the same substrate. However, all results were achieved with much less preparation effort, since the carbon concentration in the films is inherently lower (less than 1% of a ML after the first h-BN preparation at ~1000 K without using oxygen cleaning cycles), whereas depleting Pd crystals of carbon is a tiresome task. Thus the use of films could be an interesting alternative to single crystals for applications.

4. Conclusions

The presented results confirm the growth of a single monolayer of boron nitride on Pd(1 1 1), i.e. no complex structure like on Rh(1 1 1) is formed. There are two preferential orientations of the BN overlayer, one which is aligned to the substrate and one rotated by 30°, but a systematic dependence of the abundance distribution has not been found. STM measurements show Moiré patterns with different periodicities, depending on the rotation angle between the overlayer and the substrate. These results clearly show that the lattice mismatch, which is an important driving factor for the nanomesh formation on Rh(1 1 1), is not the only key ingredient for explaining the different boron nitride structures. The lattice mismatch of h-BN on Rh(1 1 1) and Pd(1 1 1) is comparable (−7% and −9%) and yet on Pd no nanomesh is observed. An explanation might be found from the comparison to the ammonia molecule adsorption. Bligaard et al. [16] calculated the dissociative chemisorption energy for the ammonia molecule on transition metal surfaces relative to the dissociation energy of the free molecule. They observe a change of 0.64 eV from the free molecule to the Pd surface in contrast to −0.61 eV for Rh. This indicates a stronger bonding of the nitrogen to Rh as compared to Pd, which is in line with the formation of a closed monolayer on Pd due to the weak adsorbate–substrate interaction, while on Rh the nitrogen might anchor more strongly to preferential sites (lock-in) and thus promote the mesh formation.

The relative structure abundance might be traced back to an interplay between lattice mismatch and lock-in energy arguments [4]. As shown by Grad et al. [12], the preferential site for N atoms on Ni(1 1 1) is the top site, while configurations with N on other sites are not stable. It is likely that this is still true for Pd(1 1 1), because also for ammonia the preferential bonding site of N is the top site on this surface [17]. The number of N atoms on top sites depends on the size of the unit cell of the superstructure. While the 10×10-structure contains 121 BN units, the structure rotated by 30° must be strained or compressed to form a coincidence lattice, and the number of N atoms on the top site depends on the coincidence periodicity. As mentioned above, the lattice mismatch between the BN ring diameter and the substrate is reduced to 5.1%. Therefore the most simple structure with N on top would be a $\sqrt{3} \times \sqrt{3}$-R30°-superstructure with the BN units rotated by 30° with respect to the substrate. Despite its high number of N atoms sitting on top sites (a quarter of the N atoms in the unit cell), which implies a high lock-in energy gain, this structure is not observed in the LEED because the lattice mismatch is too high and the lock-in energy gain per N atom is small for Pd(1 1 1). Therefore the 10×10 structure with its lattice mismatch of only 0.1% is dominant, while the structure rotated by 30° appears to be incommensurate.

Furthermore, the use of thin films has been examined. The results suggest that films are a viable substitute to single crystals for studying boron nitride layers.

Acknowledgements

The authors would like to thank M. Klöckner for technical support, H.R. Scherrer (ETH Zürich) for the production of the Pd thin films and Peter Blaha (TU Vienna) for fruitful discussions. This work was supported by the Swiss National Science Foundation and by the European Union's Sixth Framework Programme via the Nanomesh project (NMP4-CT-2004-013817).

References

[1] M. Corso, W. Auwärter, M. Muntwiler, A. Tamai, T. Greber, J. Osterwalder, Science 303 (2004) 217.
[2] A. Nagashima, N. Tejima, Y. Gamou, T. Kawai, C. Oshima, Phys. Rev. Lett. 75 (1995) 3918.
[3] R.M. Desrosiers, D.W. Greve, A.J. Gellman, Surf. Sci. 382 (1997) 35.
[4] T. Greber, L. Brandenberger, M. Corso, A. Tamai, J. Osterwalder, J. Surf. Sci. Nanotech. 4 (2006) 410.
[5] M.T. Paffett, R.J. Simonson, P. Papin, R.T. Paine, Surf. Sci. 232 (1990) 286.
[6] F. Müller, K. Stöwe, H. Sachdev, Chem. Mater. 17 (2005) 3464.
[7] A.B. Preobrajenski, A.S. Vinogradov, N. Mårtensson, Surf. Sci. 582 (2005) 21.
[8] M. Corso, T. Greber, J. Osterwalder, Surf. Sci. 577 (2005) 78.
[9] T. Greber, O. Raetzo, T.J. Kreutz, P. Schwaller, W. Deichmann, E. Wetli, J. Osterwalder, Rev. Sci. Instrum. 68 (1997) 4549.
[10] W. Auwärter, T.J. Kreutz, T. Greber, J. Osterwalder, Surf. Sci. 429 (1999) 229.
[11] T.A. Land, T. Michely, R.J. Behm, J.C. Hemminger, G. Comsa, Surf. Sci. 264 (1992) 261.
[12] G.B. Grad, P. Blaha, K. Schwarz, W. Auwärter, T. Greber, Phys. Rev. B 68 (2003) 085404.
[13] E.D.L. Rienks, N. Nilius, H.P. Rust, H.J. Freund, Phys. Rev. B 71 (2005) 242404.
[14] M. Pivetta, F. Patthey, M. Stengel, A. Baldereschi, W.-D. Schneider, Phys. Rev. B 72 (2005) 115404.
[15] W. Auwärter, T.J. Kreutz, T. Greber, J. Osterwalder, Surf. Sci. 429 (1999) 229.
[16] T. Bligaard, J.K. Nørskov, S. Dahl, J. Matthiesen, C.H. Christensen, J. Sehested, J. Catal. 224 (2004) 206.
[17] S. Stolbov, T. Rahman, J. Chem. Phy. 123 (2005) 204716.